Journal of Magnetic Resonance **157,** 200–209 (2002)
doi:10.1006/jmre.2002.2586

Measurement of Small One-Bond Proton–Carbon Residual Dipolar Coupling Constants in Partially Oriented ^{13}C Natural Abundance Oligosaccharide Samples: Analysis of Heteronuclear $^{1}J_{CH}$-Modulated Spectra with the BIRD Inversion Pulse

Tran Nghia Pham,* Tibor Liptaj,*,[1] Krystyna Bromek,† and Dušan Uhrín†,[1]

*Slovak University of Technology, Faculty of Chemical and Food Technology, Central Laboratories, Radlinského 9, 812 37 Bratislava, Slovakia; and †University of Edinburgh, Department of Chemistry, Joseph Black Building, West Mains Rd., Edinburgh EH9 3JJ, Scotland, United Kingdom

Received January 7, 2002; revised June 10, 2002

Two 2D *J*-modulated HSQC-based experiments were designed for precise determination of small residual dipolar one-bond carbon–proton coupling constants in ^{13}C natural abundance carbohydrates. Crucial to the precision of a few hundredths of Hz achieved by these methods was the use of long modulation intervals and BIRD pulses, which acted as semiselective inversion pulses. The BIRD pulses eliminated effective evolution of all but $^{1}J_{CH}$ couplings, resulting in signal modulation that can be described by simple modulation functions. A thorough analysis of such modulation functions for a typical four-spin carbohydrate spin system was performed for both experiments. The results showed that the evolution of the ^{1}H–^{1}H and long-range ^{1}H–^{13}C couplings during the BIRD pulses did not necessitate the introduction of more complicated modulation functions. The effects of pulse imperfections were also inspected. While weakly coupled spin systems can be analyzed by simple fitting of cross peak intensities, in strongly coupled spin systems the evolution of the density matrix needs to be considered in order to analyse data accurately. However, if strong coupling effects are modest the errors in coupling constants determined by the "weak coupling" analysis are of similar magnitudes in oriented and isotropic samples and are partially cancelled during dipolar coupling calculation. Simple criteria have been established as to when the strong coupling treatment needs to be invoked.

Key Words: **residual dipolar coupling constants; *J*-modulated HSQC; one-bond carbon–proton coupling constants; BIRD pulse; carbohydrates.**

INTRODUCTION

Scalar one-bond proton–carbon couplings ($^{1}J_{CH}$) have been correlated extensively with various molecular properties and NMR parameters (*1*). During the past decade, $^{1}J_{CH}$ coupling constants have also been introduced into structural refinement of biomolecules such as carbohydrates (*2–5*), proteins (*6–8*), and oligonucleotides (*9*). More recently, the appearance of various residual dipolar couplings in high-resolution NMR spectra, as a result of a partial orientation of molecules (*10, 11*), has further increased interest in techniques for measurement of one-bond heteronuclear splittings.

Existing techniques for measurement of coupling constants can be divided into three basic categories: *J*-coupled methods, quantitative *J*-correlation, and *J*-modulated experiments. The first category of experiments use the directly or indirectly detected dimensions of 2D or 3D spectra to record heteronuclear splittings (*12–16*), often in combination with spin-state selection to simplify spectra (*17–22*), or the E.COSY principle (*23*). Coupling constants are determined from the difference in resonance frequencies of multiplets. In quantitative *J*-correlation (*24, 25*) the coupling constants are calculated from cross peak intensities measured in two heterocorrelated spectra. In the first the effect of the measured coupling constant is eliminated while in the second the couplings are allowed to modulate cross peak intensities. In *J*-modulated experiments (*26–32*) a series of spectra are acquired. The cross peak intensities are quantified and the coupling constants determined with very high precision (*30*) by fitting procedures using appropriate modulation functions.

Residual dipolar couplings observed in moderately oriented liquid crystalline media are determined as the difference between the total coupling (we denote it as K) observed in the oriented and nonoriented samples, $D = K_{\text{orient}} - K_{\text{non-orient}} = (J + D) - J$. For very weakly oriented samples exhibiting small dipolar couplings (~2 Hz), the *J*-modulation methods are likely necessary, while for more strongly oriented systems, with larger dipolar couplings, the techniques from the first two categories will suffice. While the majority of measurements of heteronuclear dipolar couplings so far have been performed on isotope-labeled biomolecules, one-bond residual proton–carbon coupling constants have been measured on ^{13}C natural abundance carbohydrate (*16, 33–35*) and DNA samples (*36–38*) using t_1 or t_2-coupled 2D HSQC experiments.

[1] To whom correspondence may be addressed. E-mail: liptaj@chtf.stuba.sk, dusan@chem.ed.ac.uk.

1090-7807/02 $35.00

In this work we present and analyze the J-modulated 2D HSQC-based methods designed for the determination of small one-bond carbon–proton dipolar coupling constants ($^1D_{CH}$) in ^{13}C natural abundance carbohydrates. Due to the near-parallel orientation of all C–H_{ax} bonds in hexapyranose rings the $^1D_{CH}$ coupling constants are usually not sufficient for quantification of the alignment and need to be supplemented by more abundant proton–proton residual dipolar couplings (D_{HH}). A high degree of magnetic orientation may be detrimental for the measurement of D_{HH} couplings due to the unresolved multiplets caused by appearance of numerous proton–proton dipolar couplings and the possibility of induced strong coupling effects. A possible solution is to use only weak alignment forces in combination with precise methods for measurement of small $^1D_{CH}$ and D_{HH} (*39*) coupling constants. Such methods are presented in this paper using a model trisaccharide (**I**):

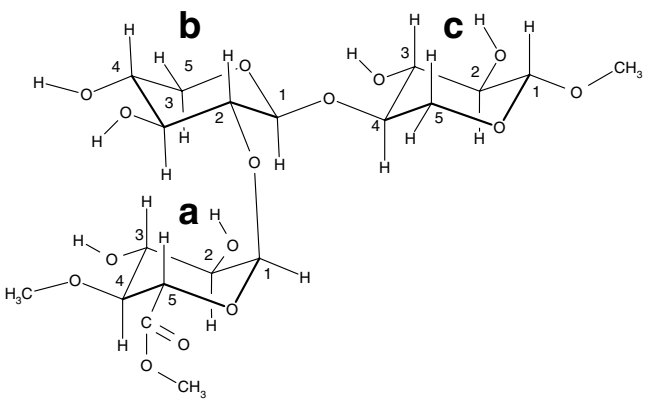

RESULTS AND DISCUSSION

Two 2D J-modulated HSQC-based methods are proposed for the measurement of $^1K_{CH}$ coupling constants. Both use a double INEPT transfer of magnetization and pulsed field gradients for coherence selection. A principal difference between the two techniques is in the position of the modulation period. In the pulse sequence of Fig.1a the modulation period is in place of a regular preparation period i.e., when the magnetization is on protons. In the pulse sequence of Fig.1b the modulation is placed after the initial INEPT step, i.e., when the magnetization is on carbon. The techniques are referred to here as jch_h and jch_c, with the last letter indicating the position of the modulation period. The jch_c expriment shows some analogy with two J-modulated experiments proposed for measurement of $^1D_{NH}$ and $^1D_{CH}$ couplings in isotopically enriched proteins. A novel element of this work is the suppression of the evolution of long-range coupling constants by a BIRD^{d,X} pulse (*40, 41*) applied amid the modulation periods of both jch_c and jch_h experiments. Different long-range interactions are refocused, depending on where the magnetization is at the time of the application of the BIRD pulse. When on protons, the overall effect is refocusing of proton–proton couplings of ^{13}CH groups, while the same BIRD^{d,X} pulse eliminates long-range proton–carbon interactions when the magnetization is on carbons. Removal of these long-range interactions allows the use of long J-modulation intervals during which the $^1K_{CH}$ coupling constants can be sampled with high accuracy: the longer the modulation period, the better are the small differences between the $^1K_{CH}$ coupling constants translated into the experimental intensities of observed cross peaks. The relaxation effects are thus the only limiting factor for setting the length of the modulation period. The situation is slightly more complicated for CH_2 groups in the jch_h method, where the evolution of geminal proton–proton coupling constants is not suppressed by the BIRD pulse. In order to minimize the effects of $^2J_{HH}$ couplings and maximize the cross peak intensities, the length of the modulation period in this experiment must be centered around the time points of $n/^2J_{HH}$ ($n = 1, 2, 3 \ldots$). When this condition is obeyed, the jch_h experiment allows determination of both $^1J_{CH}$ coupling constants of CH_2 groups with nonequivalent protons, while only their sum

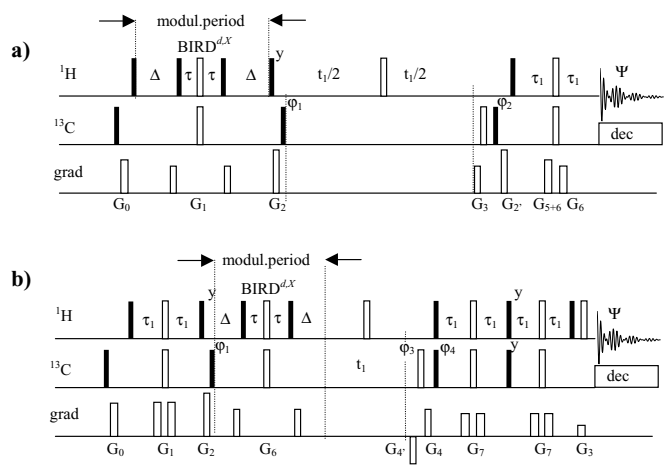

FIG. 1. Pulse sequences for (a) jch_h and (b) jch_c experiments. Both use pulsed field gradients for coherence selection. Experiment (b) is sensitivity enhanced (43). Thick and thin rectangles represent 90° and 180° pulses, respectively. Unless stated otherwise pulses were applied from the x axis. The following phase cycling was used: $\varphi_1 = x, -x$; $\varphi_2 = x, x, -x, -x$; $\varphi_3 = x, x, y, y, -x, -x, -y, -y$; $\varphi_4 = x$; $\Psi = x, -x, -x, x$. Delay 2Δ is the variable modulation time, $\tau_1 = 0.25/^1J_{CH}$, and $\tau = 0.5/^1J_{CH}$. The BIRD pulse was optimized for $^1J = 155$ Hz. In experiment (a) the States–TPPI method was employed for sign discrimination in F_1; the phase φ_1 was incremented by 90° during the acquisition of imaginary t_1 points together with the sign inversion of the gradient G_3. All gradients were 1 ms long and had the following strengths: $G_0 =$ 11 G/cm, $G_1 = 7.5$ G/cm, $G_2 = 22$ G/cm, $G_3 = 24$ G/cm, $G_{2'} = -20$ G/cm, $G_5 = 6.06$ G/cm, $G_6 = 9$ G/cm. G_3 and G_5 were used as coherence selection gradients. In experiment (b) the phase φ_4 was incremented by 180° during the acquisition of imaginary t_1 points together with the sign inversion of the gradient G_3. All gradients, except for the coherence selection gradients, were 0.4 ms long. The gradients $G_{4'}$, G_4, and G_3 were set to 1.25, 1.25, and 0.311 ms, respectively. The strength of gradients was $G_{4'} = -15$ G/cm, $G_4 = 15$ G/cm, $G_3 = 30$ G/cm, and $G_7 = 6$ G/cm. G_4 and G_3 were used as coherence selection gradients. All spectra were processed using the protocol for sensitivity-enhanced techniques.

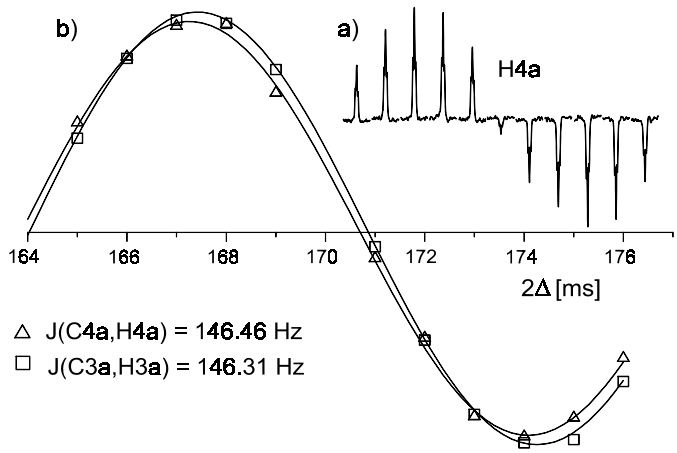

FIG. 2. (a) Traces through the $H_{4a}C_{4a}$ cross-peaks from a series of spectra acquired using the *jhc_h* pulse sequence of Fig. 1a. (b) fitting of cross peak intensities (Eq. [7]) derived from signals of two protons with very similar $^1J_{CH}$ coupling constants.

is available from the *jch_c* spectra. The *jch_c* experiment can therefore be considered as an experiment designed specifically for CH groups and its sensitivity can be improved by incorporation of the sensitivity-enhanced INEPT transfer step, which is less effective for CH_2 groups (*42, 43*).

With a large spread of $^1J_{CH}$ coupling constants and long modulation intervals it is important to choose a set of modulation intervals which yields an even distribution of signal intensities regardless of the actual value of the coupling constant. For this a time interval of approximately 12 ms is required. The resolution capability of J-modulated methods is illustrated in Fig. 2 using coupling constants $^1J_{C_{4a},H_{4a}}$ and $^1J_{C_{3a},H_{3a}}$, which differ only by 0.15 Hz. Nevertheless, this difference is clearly visible in the cross peak intensities (Fig. 2b) obtained from the *jch_h* spectra, which were acquired using a modulation period of 170 ± 6 ms.

If such small differences are detectable experimentally, care must be taken to analyze data rigorously. As the modulation interval contains a BIRD pulse, rather than a simple pair of 180° pulses (29), we have focused our attention on this pulse sequence element as a possible source of systematic errors. Starting with an ideal BIRD approximation we have described the effects of nonideal BIRD pulses on weakly coupled spins using the product spin operator formalism (*44*). As carbohydrates are notorious for the occurrence of strong couplings we have also developed an analysis based on the evolution of the density matrix, which overcomes the limitations of the weak coupling approximation.

Data Analysis of Weakly Coupled Spin Systems

In the ideal BIRD pulse, delay τ between the pulses of the BIRD cluster is set exactly to $0.5/^1K_{CH}$, no evolution of proton–proton or long-range proton–carbon couplings is allowed, and perfect inversion of relevant spins is achieved. Using these assumptions the following equations describe the signal intensities as a function of the modulation period, 2Δ, in the *jch_h* experiment,

$$I_{CH} = I^0_{CH} \sin\left(\pi\, {}^1K_{CH} 2\Delta\right) \exp(-2\Delta/T_2) \quad [1]$$

$$I_{CH_2} = I^0_{CH_2} \sin\left(\pi\, {}^1K_{CH} 2\Delta\right) \cos\left(\pi^2 K_{HH} 2\Delta\right) \times \exp(-2\Delta/T_2) \quad [2]$$

$$I_{CH_3} = I^0_{CH_3} \sin\left(\pi\, {}^1K_{CH} 2\Delta\right) \exp(-2\Delta/T_2), \quad [3]$$

where $I^0$is the amplitude factor, K is either J or $J + D$, standing for the scalar and the sum of scalar and dipolar coupling constants, respectively, and T_2 is the effective spin–spin relaxation time.

Similar equations can be derived for cross peak intensities in the *jch_c* experiment:

$$I_{CH} = I^0_{CH} \cos\left(\pi\, {}^1K_{CH} 2\Delta\right) \exp(-2\Delta/T_2) \quad [4]$$

$$I_{CH_2} = I^0_{CH_2} \cos\left[\pi\left({}^1K_{CH_a} + {}^1K_{CH_b}\right)2\Delta\right] \exp(-2\Delta/T_2) \quad [5]$$

$$I_{CH_3} = I^0_{CH_3} \cos\left(\pi\, {}^1K_{CH} 2\Delta\right)\left[3\cos^2\left(\pi\, {}^1K_{CH} 2\Delta\right) - 2\right] \times \exp(-2\Delta/T_2). \quad [6]$$

In real spin systems, deviations from an ideal state occur because of variation of one-bond carbon–proton couplings and evolution of proton–proton and long-range proton–carbon couplings during the BIRD pulses. Modulation functions for *jch_h* and *jch_c* experiments, which take into account these effects in a typical four-spin system of carbohydrates, are given in the Appendix. Each modulation function is a sum of two contributions, *direct* and *transferred*, originating on protons attached to ^{13}C and on remote protons coupled to the ^1H–^{13}C pair, respectively. The transferred part of the function arises due to the evolution of proton–proton and long-range proton–carbon couplings during the BIRD pulse and the presence of 90° ^1H pulses which can act as polarization transfer pulses.

Initially, we will focus only on the effects of a mismatch between the actual $^1K_{CH}$ and an average value ($^1K^{ave}_{CH} = 155$ Hz), used to calculate the delay $\tau (= 0.5/{}^1K^{ave}_{CH})$, and neglect evolution of long-range couplings during the BIRD pulse. An approximate modulation function of the *jch_h* experiment and CH groups is then obtained by setting $J_1 \neq 0$, $J_{i>1} = 0$ in Eq. [A.1]:

$$I_{CH} = I^0_{CH}\left[0.5\left(1 - \cos\left(\pi\, {}^1K_{CH} 2\tau\right)\right)\right] \sin\left(\pi\, {}^1K_{CH} 2\Delta\right) \times \exp(-2\Delta/T_2) \quad [7]$$

$$= A \sin\left(\pi\, {}^1K_{CH} 2\Delta\right) \exp(-2\Delta/T_2).$$

This modulation function differs from the corresponding ideal BIRD modulation function (Eq. [1]) only in the scaling factor, $A = I^0_{CH} 0.5 * (1 - \cos(\pi\, {}^1K_{CH}/{}^1K^{ave}_{CH}))$. Therefore the only consequence of the $^1K_{CH}$ mismatch is an overall decrease of signal intensities. For a difference between the set and actual

coupling constant of <10% this drop is less then 3% and is of little significance. The approximate modulation function for a CH_2 group has a similar structure (Eq. [A.1], $J_1 \neq 0$, $J_4 = {}^1K_{CH}^{ave}$, $J_{i>1} = 0$):

$$\begin{aligned} I_{CH_2} &= I^0_{CH_2}\left[0.5\left(1 - \cos\left(\pi {}^1K_{CH} 2\Delta\right)\right)\right] \sin\left(\pi {}^1K_{CH} 2\Delta\right) \\ &\quad \times \cos\left(\pi^2 K_{HH} 2\Delta\right) \exp(-2\Delta/T_2) \qquad [8] \\ &= A \sin\left(\pi {}^1K_{CH} 2\Delta\right) \cos\left(\pi^2 K_{HH} 2\Delta\right) \exp(-2\Delta/T_2). \end{aligned}$$

An analogous approximate modulation function can be obtained for CH groups in the *jch_c* experiment by using Eq. [A.3] and $J_1 \neq 0$, $J_{i>1} = 0$,

$$\begin{aligned} I_{CH} &= I^0_{CH}\left\{\cos^2\left(\pi {}^1K_{CH}\Delta\right) + \sin^2\left(\pi {}^1K_{CH}\Delta\right)(1+c)\right\} \\ &\quad \times \exp(-2\Delta/T_2), \qquad [9a] \end{aligned}$$

where $c = \cos(\pi {}^1K_{CH} 2\tau)$. Equation [9a] can be rearranged as

$$\begin{aligned} I_{CH} &= I^0_{CH}\left\{[1 - 0.5(1+c)] \cos\left(\pi {}^1K_{CH} 2\Delta\right) + 0.5(1+c)\right\} \\ &\quad \times \exp(-2\Delta/T_2) \qquad [9] \\ &= A\left[\cos\left(\pi {}^1K_{CH} 2\Delta\right) + B\right] \exp(-2\Delta/T_2), \end{aligned}$$

where $A = I^0_{CH}[1 - 0.5(1+c)]$ and $B = 0.5(1+c)/[1 - 0.5(1+c)]$. This approximate modulation function differs from the corresponding ideal BIRD modulation function (Eq. [4]) not only in the scaling factor, but also in containing a zero-frequency component.

In the next step, the approximate modulation functions given by Eqs. [7]–[9] are tested as to how well they reproduce the synthetic data generated by exact modulation functions (Eq. [A.1] + [ΣA.2] or [A.3] + [ΣA.4]) when nonzero values of long-range coupling constants are used. The results of this analysis are presented in more detail in the Appendix. Here it suffices to say that Eq. [7] reproduced the data generated by exact modulation function (*jch_h*, CH groups, Eq. [A.1] + [ΣA.2]) within ±1%. Fitting the synthetic data of the *jch_c* experiment (CH groups, Eq. [A.3] + [ΣA.4]) by Eq. [9] yielded identical intensities within ±0.3%. When the modulation period, 2Δ, was centred on time points $n/^2J_{HH}$, Eq. [8] reproduced the exact modulation function for the CH_2 groups and *jch_h* experiment (Eq. [A.1] + [ΣA.2]) with intensity differences of <2% over a 12-ms modulation period. Such variations are likely to be hidden in the noise for natural abundance ^{13}C samples. We therefore conclude that Eqs. [7]–[9] are sufficient approximations to the corresponding exact modulation functions of *jch_c* and *jch_h* experiments. As only the sum of the $^1J_{CH}$ couplings is obtained in the *jch_c* experiment for CH_2 groups the effects of a nonideal BIRD pulse were not analyzed for this case. The couplings of the CH_3 groups were not discussed at all, mainly due to their limited scope of application in carbohydrates.

Different types of deviations from an ideal BIRD arise from miscalibration, off-resonance effects, and/or rf pulse inhomogeneity of pulses in the BIRD cluster. Such effects are more pronounced for 180° than for 90° pulses; therefore only effects of varying flip angles α and β of the central (nominally 180°) ^1H and ^{13}C pulses on the modulation functions are considered here. It can be easily shown that the result is a signal attenuation by the factor $0.25[1-\cos(\alpha)][1-\cos(\beta)]$ for both experiments. In addition, in the *jch_c* experiment a zero frequency component is introduced into the modulation function. As the zero frequency component is already incorporated into the modulation function of the *jch_c* experiment (Eq. [4]), no further modifications were required. Analogous results were obtained by Tjandra *et al.* (*29*) in a similar *J*-modulated experiment containing a simple pair of 180° pulses amid the evolution period.

It is interesting to note that the zero frequency component has appeared repeatedly during our analysis of modulation functions in the *jch_c* but not in the *jch_h* experiment. The origin of this phenomenon is that while in the *jch_h* experiment the desired magnetization is evolving during the modulation period from inphase to antiphase, in the *jch_c* experiment the original antiphase magnetization is preserved. The different mathematical identities associated with cosine and sine functions result in deviations from an ideal state appearing as an additional scaling factor in the *jch_h* experiment, while a zero frequency component appears in the *jch_c* data. By incorporating the zero frequency component into the modulation function of the *jch_c* spectra we have obtained improved fits; e.g., fitting intensities of the H1a proton signal using Eq. [4] gave $J = 176.19 \pm 0.08$, while 176.23 ± 0.03 was obtained using Eq. [9].

After considering various effects of real BIRD pulses, we can conclude that Eqs. [7]–[9] are sufficient approximations of the exact modulation functions for *jch_c* and *jch_h* experiments. As an example, coupling constants of ring **a** of the trisaccharide **I** in isotropic and oriented media were determined for *jch_h* and *jch_c* experiments (Table 1). The results obtained by both methods yielded very similar values of coupling constants with standard deviations of 0.01–0.06. Slightly higher standard deviations of coupling constants obtained from the *jch_c* experiment were due to the fact that fewer points were acquired in this experiment with fewer scans per 2D increment. For comparison, data obtained from carbon-coupled 2D HSQC spectra are also presented. The precision of these data was estimated to be ~0.2Hz. Similar results obtained in all experiments indicated that there are no systematic deviations between intensity-based and carbon-coupled methods.

Data Analysis of Strongly Coupled Spin Systems

Carbohydrates often feature strong couplings either in ^1H or ^1H–^{13}C satellite spectra even at high magnetic fields. Such effects were clearly visible in ^1H–^{13}C satellite spectra of the ring **b** of **I**. Cross peaks of H_{2b}, H_{3b}, and H_{4b} protons showed a high degree of asymmetry between their high- and low-field parts in

TABLE 1
Coupling Constants[a] [Hz] and Standard Deviations[b] of CH Groups in Ring a of I

	$^1J_{CH}$ (Isotropic sample)			$^1K_{CH}$ (Oriented sample)			$^1D_{CH} = {}^1K_{CH} - {}^1J_{CH}$		
H_i	*jch_h*	*jch_c*	HSQC[c]	*jch_h*	*jch_c*	HSQC[c]	*jch_h*	*jch_c*	HSQC[c]
1a	176.19	176.23	176.2	173.51	173.52	173.6	−2.68	−2.71	−2.6
	0.02	0.06		0.02	0.06		0.03	0.08	
2a	144.03	144.02	144.2	146.69	146.68	146.8	2.66	2.66	2.6
	0.01	0.03		0.02	0.03		0.02	0.04	
3a	146.31	146.40	146.2	148.96	149.14	149.0	2.65	2.64	2.8
	0.02	0.03		0.02	0.03		0.03	0.04	
4a	146.49	146.46	146.2	149.26	149.21	149.1	2.77	2.75	2.9
	0.03	0.04		0.02	0.04		0.04	0.06	
5a	153.87	153.77	153.7	156.51	156.50	156.3	2.64	2.73	2.6
	0.02	0.02		0.01	0.02		0.02	0.03	

[a] Determined by a nonlinear fitting of cross peak intensities using Eqs. [7] and [9] for the *jch_h* and *jch_c* data, respectively.

[b] Error bounds for the $^1D_{CH}$ couplings were calculated as the square roots of sums of the squares of standard deviations of coupling constants in isotropic and oriented media.

[c] Estimated error of 0.2 Hz; this translated into as error of 0.28 Hz for $^1D_{CH}$ couplings determined from the HSQC experiments.

F_2 carbon-coupled HSQC spectra, which precluded reliable determination of $^1J_{CH}$ coupling constants. In the following we will demonstrate that it is possible to determine $^1J_{CH}$ from *jch_c* and *jch_h* spectra in the presence of strong couplings. For this we adopt an approach developed by Morris *et al.* (*45*) for the analysis of strong coupling effects in semiselective 2D *J*-resolved experiments which incorporates BIRD pulses amid an evolution interval. During such analyses the $^1K_{CH}$ values are allowed to vary within a certain range around the weak coupling approximation value and cross peak intensities are calculated for each modulation time using Eq. [10] or [11], which are given in the Experimental section. The best fit between the theoretical and experimental cross peak intensities identifies the correct coupling constant. While identical values of $^1J_{CH}$ were obtained using this treatment and Eq. [7] for a weakly coupled spin system H_{4a}–H_{5a}–C_{5a} (Fig. 3a), for a strongly coupled system H_{2b}–H_{3b}(C_{3b})–H_{4b} the experimental data were reproduced by markedly different $^1J_{CH}$ couplings depending on the nature of the analysis. A comparison of $^1D_{CH}$ values obtained using the weak and strong coupling analyses for a more extensive data set (Table 2) indicated that in systems with modest strong coupling effects accurate dipolar couplings could still be obtained using the weak coupling approximation. In these instance the strong coupling contributions are very similar in both media and therefore cancel out when the residual coupling constants are calculated as a difference between the two one-bond splittings. The severity of the strong coupling effects in the ^{13}C satellite spectra can be classified using the ratio $R = (\Delta\delta - 0.5^1J_{CH})/J_{HH}$,

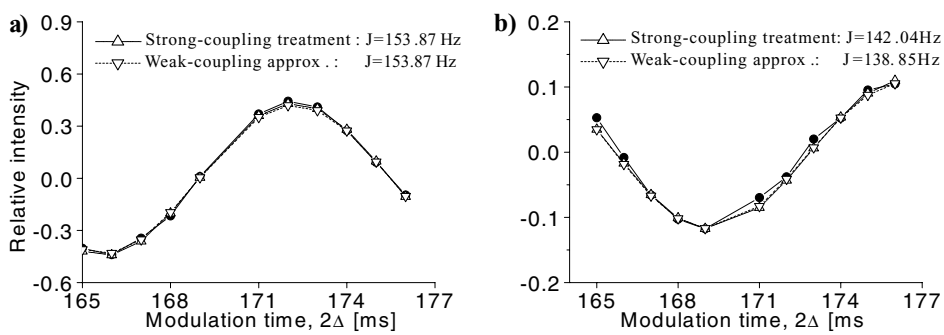

FIG. 3. The density matrix treatment of cross peak intensities. The experimental (●, *jch_h* experiment, isotropic sample) and theoretical intensities considering strong (△) and weak (▽) couplings are shown. (a) Weakly coupled spin system H_{4a}–H_{5a}–C_{5a}. The best fit of the experimental data was obtained for $^1J_{CH} = 153.87$ Hz using both weak (Eq. [7]) and strong coupling treatments. The following parameters were used for the density matrix calculation: $\delta_{4a} = 1865$; $\delta_{5a} = 2706$; $^3J(H_{4a}, H_{5a}) = 10.2$ Hz; $^2J(C_{5a}, H_{4a}) = 5.2$ Hz. (b) Strongly coupled spin system H_{2b}–H_{3b}(C_{3b})–H_{4b}. The following parameters were used for the density matrix calculation: $\delta_{2b} = 1874$; $\delta_{3b} = 1955$; $\delta_{4b} = 2035$; $^3J(H_{2b}, H_{3b}) = 9.4$ Hz; $^3J(H_{3b}, H_{4b}) = 9.2$ Hz; $^2J(C_{3b}, H_{2b}) = 5.2$ Hz; $^2J(C_{3b}, H_{4b}) = 4.1$ Hz. Both strong and weak coupling analysis reproduced the experimental data well; however, this fit was achieved by markedly different $^1J_{CH}$ coupling constants. Lower relative intensity in (b) compared with (a) is due to the strong coupling effects.

TABLE 2
Effect of Strong Couplings in the *jch_h* Experiment[a]

		Isotropic sample			Oriented sample			Dipolar couplings		
H_I	$R=(\Delta\delta-0.5^1J_{CH})/J_{HH}$	$^1K_{CH}$ weak	$^1K_{CH}$ strong	Δ^1K_{CH}	$^1K_{CH}$ weak	$^1K_{CH}$ strong	Δ^1K_{CH}	$^1D_{weak}$	$^1D_{strong}$	Δ^1D_{CH}
1a	249.3	176.19	176.19	0.00	173.51	173.51	0.00	−2.68	−2.68	0.00
2a	252.9; 5.0	144.03	144.37	0.34	146.69	147.07	0.38	2.66	2.70	0.04
3a	4.9; 21.0	146.31	146.66	0.35	148.96	149.36	0.40	2.65	2.70	0.05
4a	21.0; 72.7	146.49	146.51	0.02	149.26	149.31	0.05	2.77	2.80	0.03
5a	72.4	153.87	153.87	0.00	156.51	156.52	0.01	2.64	2.65	0.01
1b	84.4	163.32	163.32	0.00	165.71	165.72	0.01	2.39	2.40	0.01
2b	85.5; 0.79	144.01	145.99	1.98	146.90	148.96	2.06	2.89	2.97	0.08
3b	1.08; 0.99	138.85	142.04	3.19	141.28	144.81	3.53	2.43	2.77	0.34
4b	0.77; 11.7; 25.9	142.75	145.94	3.19	145.10	148.65	3.55	2.35	2.71	0.36
$5b_{ax}$	30.8, 11.8	141.61	141.72	0.11	143.55	143.67	0.12	1.94	1.95	0.01
$5b_{eq}$	30.5, 25.3	151.69	151.72	0.03	151.28	151.30	0.02	−0.41	−0.42	−0.01

[a] $R=(\Delta\delta-0.5^1J_{CH})/J_{HH}$ classifies the severity of the strong coupling. $\Delta\delta$ is the chemical shift difference of coupled protons. R was calculated for proton pairs i, $i-1$ and i, $i+1$; weak and strong refer to coupling constants [Hz] obtained using Eqs. [7], [8], and [11], respectively. Δ^1K_{CH} and Δ^1D_{CH} give the difference between values obtained by the weak and strong coupling treatment of the data.

where $\Delta\delta$ is the chemical shift difference of coupled protons and J_{HH} is the homonuclear coupling constant. In order to determine the limits in which the weak coupling approximation is adequate a series of simulations was performed using the H_{2b}–H_{3b}($^{13}C_{3b}$)–H_{4b} spin system. This is an AB(X)C spin system with strong couplings between AB and BC spins. The cross peak intensities of H_{3b} simulated for the *jch_c* experiment using Eq. [10] were subjected to weak coupling analysis using Eq. [9]. Figure 4a shows the obtained one-bond splitting as a function of R. The $^1D_{CH}$ values determined as $^1K_{CH}$–$^1J_{CH}$ (Fig. 4b) reached at least 99% of the nominal dipolar coupling for $R \geq 5$, despite the fact that at $R=5$ the $^1J_{CH}$ and $^1K_{CH}$ values differed by 0.6 Hz from the true one-bond splitting. For AB(X)M spin systems, with only one pair of strongly coupled protons, the weak coupling approximation yielded accurate values of $^1D_{CH}$ for $R \geq 3$. Similar results were obtained for the *jch_h* experiment (data not shown).

It should be noted that the density matrix treatment requires a full description of spin systems including accurate proton chemical shifts, proton–proton and long-range proton–carbon coupling constants, and an estimate of the effective relaxation time. Our simulations indicate that for the *jch_h* experiments only values of proton–proton couplings were critical. Setting the long-range proton–carbon couplings to zero did not have any effect. In the *jch_c* data the heteronuclear $^2J_{BX}$ couplings were also important and values differing by 1.0 Hz produced variations in $^1J_{CH}$(±0.2 Hz) for a spin system with $R < 1.5$. Nevertheless, it is possible to use this type of data analysis routinely, as accurate

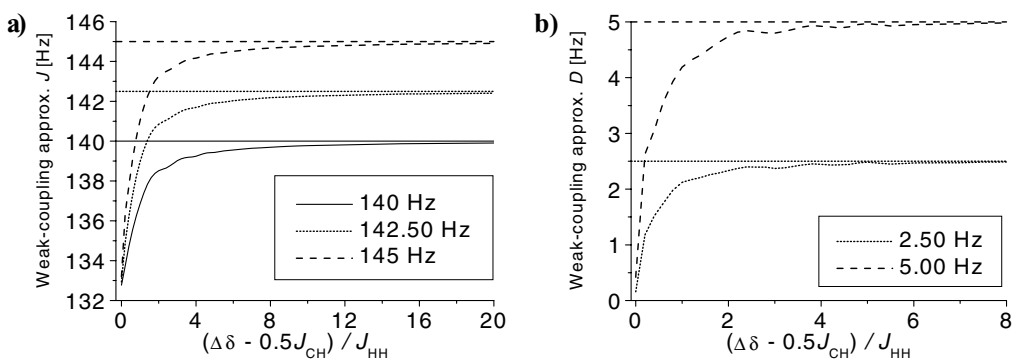

FIG. 4. Determining the limits of the weak coupling treatment. (a) The $^1J_{CH}$ couplings as a function of $(\Delta\delta-0.5^1J_{CH})/J_{HH}$ obtained when the cross peak intensities calculated using the strong coupling formalism (Eq. [10]) were analyzed in the weak coupling approximation (Eq. [9]). Strongly coupled spin system H_{2b}–H_{3b}(C_{3b})–H_{4b} was used with $^1J_{CH}$ of 140.00 Hz and $^1K_{CH}$ of 142.50 or 145.00 Hz, which yielded dipolar couplings of 2.50 or 5.00 Hz. Other parameters of this spin system are given in the caption of Fig. 3. Chemical shifts of protons H_{2b} and H_{4b} were initially positioned in the middle of the high- and low-field one-bond satellites of proton H_{3b} ($\Delta\delta=0$), respectively. The chemical-shift difference, $\Delta\delta$, was gradually increased by keeping the chemical shift of the H_{3b} proton fixed, while moving the chemical shifts of protons H_{2b} and H_{4b} equidistantly towards the higher and lower fields, respectively. (b) Dipolar couplings calculated as a difference between $^1K_{CH}$ and $^1J_{CH}$ values given in the graph (a).

values of J_{HH} couplings can be obtained easily from weakly coupled ^{1}H–^{12}C spectra and values of $^2J_{CH}$ of carbohydrates are available for various monosaccharides (*46*).

EXPERIMENTAL

All spectra were acquired at 5°C on a 600-MHz INOVA NMR spectrometer equipped with a 5-mm triple-axis triple-resonance probe. The concentration of the trisaccharide sample was 5 mg/0.5 ml of D_2O or in liquid-crystalline medium. The liquid-crystalline medium was prepared from the phage *Filamentous bacteriophage fd*, wild type M13 (47) purified in centrifuge. After purification and dialysis the phage was concentrated to a density of 10×10^{14} phage/ml, which corresponds to about 10 mg of phage in 1ml. The residual quadrupolar coupling constant of D_2O was 3.6 Hz.

A series of 12 2D *jch_h* spectra were acquired using the pulse sequence of Fig.1a. For the reference spectrum Δ was set to 3.24 ms, and the remaining 11 time intervals of Δ were varied between 165 and 176 ms in 1-ms steps. The one-bond coupling constant evolution intervals were optimized for $^1J_{CH} = 155$ Hz. Sixteen transients were acquired for each of 240 complex points. The reference spectrum was inserted into the series in order to ensure good definition of the initial amplitude, allowing reliable fitting of effective relaxation times. Acquisition times were 40.3 and 170 ms in t_1 and t_2, respectively. The overall acquisition time was 48 h. For 2D *jch_c* spectra the reference spectrum was acquired with $\Delta = 6.66$ ms and seven intervals of Δ between 150 and 162 ms in steps of 2 ms were used. Eight transients were accumulated for each of 240 complex points. Acquisition times were 40.3 and 170 ms in t_1 and t_2, respectively. The overall acquisition time was 16 h. Integral intensity for each resonance in each 2D spectrum was determined by 2D integration routines available in the VNMR software.

^{13}C coupled HSQC spectra were acquired using pulse-field gradients for suppression of ^{12}C-bound protons (*48*). Two ^{13}C $90°(x)$, $90°(y, -y)$ pulses were applied at the end of the refocusing period in order to remove residual antiphase components of carbon-coupled proton multiplets. Eight transients were acquired for each of the 480 complex points. Acquisition times were 81.6 and 500 ms in t_1 and t_2, respectively. The overall acquisition time was 4 h. After regular 2D processing, traces containing signals were extracted, inverse Fourier transformed, and zero filled (0.0915 Hz/point) prior to final Fourier transformation. The high-field part of the multiplet contained in each 1D spectrum was shifted in the direction of its low field portion till the best overlay was achieved. This displacement represents the coupling constant. More accurate values were obtained in this way than by calculating the coupling constant as a difference of frequencies provided by peak picking routines. Computer-aided read-out of the coupling constants failed in the case of C_{3b}–H and C_{4b}–H spins. This was caused by the asymmetry of the C–H doublet due to strong coupling effects.

Theoretical cross peak intensities in the strong coupling treatment of the *jch_c* experiment are calculated as a sum of intensities of spectral transitions (*45*),

$$I(jch\_c)^{\text{theo}}(2\Delta) = \left(\sum_i\sum_j\sum_k\sum_l -F^y_{ij}B^*_{ik}B_{jl}F^y_{ik}e^{i\pi\nu_{ijkl}2\Delta}\right)e^{-2\Delta/T2}, \quad [10]$$

where **B** is the matrix representation of the action of the BIRD pulse and F^y represents the carbon $y-$antiphase magnetization. $\nu_{ij,kl} = 0.5(\nu_j - \nu_i + \nu_l - \nu_k)$ is the average modulation frequency of the F^y coherences, which is converted in the middle of the modulation period by the BIRD pulse from σ_{ij} into σ_{kl} coherence. ν_i is the ith energy eigenvalue of the spin system (expressed in frequency units).

In the *jch_h* experiment the initial state of the spin systems is a superposition of $-y$-inphase magnetization of all protons, $F^y = \Sigma_n F^{y,n}$, where n is a proton label. A signal observed on the nth proton is proportional to the amount of x-antiphase magnetization with respect to the directly bonded carbon at the end of the modulation period and is represented by an operator $G^{x,n}$. With this notation theoretical cross-peak intensities in the *jch_h* experiment can be expressed as

$$I_n(jch\_h)^{\text{theo}}(2\Delta) = \left(\sum_i\sum_j\sum_k\sum_l -F^y_{ij}B^*_{ik}B_{jl}G^{x,n}_{ik}e^{i\nu_{ijkl}2\Delta}\right)e^{-2\Delta/T2}. \quad [11]$$

CONCLUSIONS

Two experiments, *jch_c* and *jch_h*, presented here for precise determination of residual dipolar couplings, $^1D_{CH}$, worked equally well. The use of the latter is recommended when couplings of CH_2 groups are of interest as only the sum of $^1J_{CH}$ of geminal protons is obtained from the former experiment. On the other hand the *jch_c* experiment is two times more sensitive than the *jch_h*, as both use pulsed field gradients for coherence selection, although only the former technique uses the sensitivity enhanced protocol. The *jch_c* is a method of choice for measurement of $^1J_{CH}$ in CH groups. The in-depth analysis of the modulation period of these experiments, which contained a BIRD pulse, showed that the exploitation of the BIRD pulse as a semiselective inversion pulse has distinct advantages. It allows long modulation periods, which are necessary for very precise determination of one-bond heteronuclear coupling constants, to be used. At the same time it was shown that the BIRD pulses do not complicate the analysis of the data and simple modulation functions were derived which approximate the exact modulation functions very well. These can be used for weakly coupled spin systems with no prior knowledge of the actual spin coupling constants.

For strongly coupled spin systems the evolution of the density matrix needs to be considered in order to analyse data accurately. However, if the contributions of strong couplings are modest they do not affect the resulting values of dipolar coupling constants significantly, as these are of similar magnitudes in oriented and isotropic samples and the weak coupling approximation can be used. Simple criteria have been established as to when the strong coupling treatment needs to be invoked.

APPENDIX

The exact modulation functions of *jch_h* and *jch_c* pulse sequences for a four-spin system (Scheme 1) containing one ^{13}C (S) atom and three ^1H nuclei (I_1, I_2 and I_3) were obtained. One-scan experiments were analyzed using the pulse sequence fragment $\rho_1 - \Delta - \text{G-BIRD}^{d,X}(2\tau) - G - \Delta - \rho_2$, where ρ_1 represents coherences which are present at the beginning of the modulation period. ρ_2 is the coherence at the end of the modulation period, which is eventually converted into the observable signal; Δ is the free evolution period. CH groups were analysed assuming $J_1 = {}^1J_{CH}$ and a linear spin system with $J_6 = 0$. For CH_2 groups protons I_1 and I_2 were assumed to be directly bonded to S and $J_6 \neq 0$. Relaxation terms were omitted in all equations presented in the Appendix.

jch_h Experiment

In this experiment $\rho_1 = \Sigma_\iota - I_{iy}$ and $\rho_2 = 2I_{1x}S_z$. Contributions to ρ_2 arise from proton $I_{1y}(-I_{1y} \rightarrow 2I_{1x}S_z$, *direct contribution*) and from other protons coupled to proton $I_1(-I_{iy} \rightarrow 2I_{1x}S_z, i \neq 1$, *transferred contributions*). The direct contribution is described by the equation

$$\begin{aligned} I_1^{\text{direct}} = {} & s_{2J1\Delta} I^0 \{ c^2_{J2\Delta} c^2_{J3\Delta} [0.5(1 - c_{J1\tau} c_{J2\tau} c_{J3\tau})] \\ & + c^2_{J2\Delta} s^2_{J3\Delta} [0.5(-c_{J1\tau} c_{J2\tau} c_{J5\tau} c_{J6\tau} - s_{J1\tau} s_{J2\tau} s_{J5\tau} s_{J6\tau} \\ & + c_{J3\tau} c_{J5\tau} c_{J6\tau})] + s^2_{J2\Delta} c^2_{J3\Delta} [0.5(-c_{J1\tau} c_{J3\tau} c_{J4\tau} c_{J6\tau} \\ & - s_{J1\tau} s_{J3\tau} s_{J4\tau} s_{J6\tau} + c_{J2\tau} c_{J4\tau} c_{J6\tau})] \\ & + s^2_{J2\Delta} s^2_{J3\Delta} [0.5(c_{J2\tau} c_{J3\tau} c_{J4\tau} c_{J5\tau} \\ & + s_{J2\tau} s_{J3\tau} s_{J4\tau} s_{J5\tau} - c_{J1\tau} c_{J4\tau} c_{J5\tau})] \}, \end{aligned} \quad [A.1]$$

where $c_{Ji\Delta} = \cos(\pi J_i \Delta)$, $s_{Ji\Delta} = \sin(\pi J_i \Delta)$, $c_{Ji\tau} = \cos(\pi J_i 2\tau)$, $s_{Ji\tau} = \sin(\pi J_i 2\tau)$, $c^2_{Ji\Delta} = \cos^2(\pi J_i \Delta)$, $s^2_{Ji\Delta} = \sin^2(\pi J_i \Delta)$, $s_{2Ji\Delta} = \sin(\pi J_i 2\Delta)$, $i = 1, 2, \ldots, 6$; 2τ and 2Δ are the duration of the BIRD pulse and the modulation period, respectively.

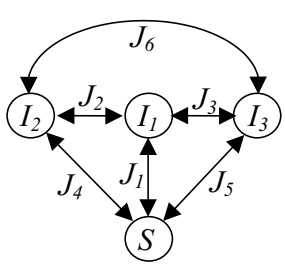

SCHEME 1

Transferred contributions are illustrated here using the transfer $-I_{2y} \rightarrow 2I_{1x}S_z$. The expressions for other protons can be derived by appropriate permutation of indices and the total transferred contribution is their sum as indicated in the text. Please note that the chemical shifts are not refocused for the transferred component. This is because the magnetization resides on different protons before (I_2) and after (I_1) the BIRD pulse,

$$\begin{aligned} I_1^{I2} = {} & I^0 c_{\nu 12\Delta} s_{J(1+4)\Delta} \{ s_{J2\Delta} c_{J2\Delta} c_{J3\Delta} c_{J6\Delta} [-0.5 s_{J2\tau} (c_{J1\tau} c_{J3\tau} \\ & + c_{J4\tau} c_{J6\tau})] + s^2_{J2\Delta} c_{J3\Delta} c_{J6\Delta} [0.5 (s_{J1\tau} c_{J3\tau} s_{J4\tau} c_{J6\tau} \\ & + c_{J1\tau} s_{J3\tau} c_{J4\tau} s_{J6\tau})] + s_{J2\Delta} c_{J2\Delta} s_{J3\Delta} s_{J6\Delta} \\ & \times [0.5 (c_{J2\tau} s_{J5\tau} (s_{J1\tau} s_{J6\tau} + s_{J3\tau} s_{J4\tau}) - s_{J2\tau} c_{J5\tau} (c_{J1\tau} c_{J6\tau} \\ & + c_{J3\tau} c_{J4\tau}))] + c^2_{J2\Delta} s_{J3\Delta} s_{J6\Delta} [-0.5 s_{J3\tau} c_{J5\tau} s_{J6\tau}] \\ & + s^2_{J2\Delta} s_{J3\Delta} s_{J6\Delta} [0.5 s_{J1\tau} s_{J4\tau} c_{J5\tau}] \}, \end{aligned} \quad [A.2]$$

where $c_{\nu 12\Delta} = \cos[\pi(\nu_1 - \nu_2)\Delta]$; ν_1 and ν_2 are chemical shifts (in Hz) of protons I_1 and I_2.

The effects of nonzero long-range couplings for CH groups were tested as follows. Theoretical cross peak intensities were calculated using a complete transfer function (Eq. [A.1] + [ΣA.2]) and a typical set of coupling constants ($J_2 = 10$, $J_3 = 8.5$; $J_4 = 6.5$, $J_5 = 3.3$ Hz, and $J_6 = 0$) as a function of Δ. In this calculation the transferred contribution from all protons was included. The data were then fit using Eq. [7]. When τ was set exactly to $0.5/{}^1K_{CH}$, Eq. [7] approximated the synthetic data within $\pm 0.2\%$. When the variations between the set and used $^1K_{CH}$ of up to 15 Hz were used, differences of up to $\pm 1\%$ were observed. As the variation of $^1K_{CH}$ in the absence of the long-range coupling constants is treated rigorously by Eq. [7], it is obvious that the increased scatter is caused by simultaneous variations of $^1K_{CH}$ couplings and inclusion of long-range couplings. This effect was not observed when only the *direct* component of the modulation function (Eq. [A.1]) was used to calculate the theoretical intensities, indicating that the *transferred* contribution is responsible for the increased, but still very small deviations. Contrary to the case for CH groups, the transferred contribution (Eq. [A.2]) in CH_2 groups can be significant and reach up to 20% of the amplitude of the direct component. However, this contribution is negligible in some parts of the modulation function. These parts coincide with the maxima of the *direct contribution* function ($n/{}^2J_{HH}$), which are used in experiments. This is not a surprising result, since the mutual antiphase magnetization of geminal protons responsible for the proton–proton transfer goes through a minimum at these points. When the modulation period, 2Δ, was centered on time points $n/{}^2J_{HH}$, Eq. [8] reproduced the theoretical data (Eq. [A.1] + [ΣA.2]) with intensity differences of $<2\%$ over

a 12-ms modulation period. During the calculation of theoretical data, the BIRD delay was optimized for $^1J = 155$ Hz and the following coupling constants were used: $J_1 = 145$; $J_2 = 12$; $J_3 = 8.5$; $J_4 = 153$; $J_5 = 5.5$; and $J_6 = 6$ Hz.

jch_c Experiment

In this experiment $\rho_1 = \Sigma_i 2I_{iz}S_y$ and $\rho_2 = 2I_{Iz}S_y$. Similarly to the *jch_h* experiment, there are two contributions to the modulation function, *direct contribution* ($2I_{Iz}S_y \rightarrow$, $2I_{Iz}S_y$) and *transferred contribution* ($2I_{iz}S_y \rightarrow 2I_{Iz}S_y$, $i \neq 1$):

$$\begin{aligned} I_1^{\text{direct}} = {} & c_{J1\Delta}^2\{c_{J4\Delta}^2 c_{J5\Delta}^2([c_{J2\tau}c_{J3\tau}c_{J4\tau}c_{J5\tau}] + [s_{J2\tau}s_{J3\tau}s_{J4\tau}s_{J5\tau}]) \\ & + c_{J4\Delta}^2 s_{J5\Delta}^2[c_{J2\tau}c_{J4\tau}] + s_{J4\Delta}^2 c_{J5\Delta}^2[c_{J3\tau}c_{J5\tau}] + s_{J4\Delta}^2 s_{J5\Delta}^2\} \\ & + s_{J1\Delta}^2\{c_{J4\Delta}^2 c_{J5\Delta}^2[c_{J1\tau}c_{J4\tau}c_{J5\tau}] + c_{J4\Delta}^2 s_{J5\Delta}^2[c_{J3\tau}c_{J1\tau}c_{J4\tau}] \\ & + s_{J4\Delta}^2 c_{J5\Delta}^2[c_{J2\tau}c_{J1\tau}c_{J5\tau}] + s_{J4\Delta}^2 s_{J5\Delta}^2[c_{J2\tau}c_{J3\tau}c_{J1\tau}]\} \end{aligned} \quad [A.3]$$

$$\begin{aligned} I_1^{12} = {} & s_{J1\Delta}c_{J1\Delta}s_{J4\Delta}c_{J4\Delta}c_{J5\Delta}^2\{-[c_{J2\tau}c_{J3\tau}c_{J4\tau}c_{J5\tau}] \\ & - [s_{J2\tau}s_{J3\tau}s_{J4\tau}s_{J5\tau}] + [c_{J3\tau}c_{J5\tau}] + [c_{J1\tau}c_{J4\tau}c_{J5\tau}] \\ & - [c_{J2\tau}c_{J1\tau}c_{J5\tau}]\} + s_{J1\Delta}c_{J1\Delta}s_{J4\Delta}c_{J4\Delta}s_{J5\Delta}^2 \\ & \times\{1 - [c_{J2\tau}c_{J4\tau}] + [c_{J3\tau}c_{J1\tau}c_{J4\tau}] - [c_{J2\tau}c_{J3\tau}c_{J1\tau}]\}. \end{aligned} \quad [A.4]$$

Since only a sum of one-bond coupling constants is obtained for CH_2 groups in this experiment, effects of proton–proton and long-range proton–carbon couplings for CH spin systems only were inspected for this pulse sequence. Theoretical cross peak intensities were calculated using a complete transfer function (Eq. [A.3] + [ΣA.4]) for a typical set of coupling constants ($J_2 = 10$, $J_3 = 8.5$; $J_4 = 6.5$, $J_5 = 3.3$ Hz and $J_6 = 0$) as a function of Δ. Very good fits were obtained using Eq. [9] with intensity differences of only ±0.3%.

ACKNOWLEDGMENT

This work was supported by the British Council and the Slovak University of Technology joint research collaboration program, the EPSRC (Grant R59496), and the Slovak Grant Agency for Science (Grant VEGA 1/9135/02). We thank G. A. Morris for a program for the analysis of strongly coupled spin systems.

REFERENCES

1. P. E. Hansen, Carbon–hydrogen spin–spin coupling constants, *Prog. NMR Spectrosc.* **14,** 175–296 (1981).
2. M. Hricovíni and I. Tvaroška, Conformational dependence of the one-bond carbon–proton coupling-constants in oligosaccharides, *Magn. Reson. Chem.* **28,** 862–866 (1990).
3. I. Tvaroška and F. R. Taravel, Carbon–proton coupling constants in the conformational analysis of sugar molecules, *Adv. Carbohyd. Chem. Biochem.* **51,** 15–61 (1995).
4. A. S. Serianni, J. Wu, and I. Carmichael, One-bond ^{13}C–^1H spin-coupling constants in aldofuranosyl rings—Effect of conformation on coupling magnitude, *J. Am. Chem. Soc.* **117,** 8645–8650 (1995).
5. C. A. Podlasek, W. A. Stripe, I. Carmichael, M. Y. Shang, B. Basu, and A. S. Serianni, ^{13}C–^1H spin-coupling constants in the β-D-ribofuranosyl ring: Effect of ring conformation on coupling magnitudes, *J. Am. Chem. Soc.* **118,** 1413–1425 (1996).
6. H. Egli and W. von Philipsborn, ^{13}C NMR spectroscopy.29. Conformational dependence of one-bond $C_\alpha H_\alpha$ spin coupling in cyclic-peptides, *Helv. Chim. Acta* **64,** 976–988 (1981).
7. D. F. Mierke, S. G. Grdadolnik, and H. Kessler, Use of one-bond $C_\alpha H_\alpha$ coupling-constants as restraints in MD simulations, *J. Am. Chem. Soc.* **114,** 8283–8284 (1992).
8. G. W. Vuister, F. Delaglio, and A. Bax, An empirical correlation between $^1J(C_\alpha H_\alpha)$ and protein backbone conformation, *J. Am. Chem. Soc.* **114,** 9647–9675 (1992).
9. G. Varani and I. Tinoco, Carbon assignments and heteronuclear coupling-constants for an RNA oligonucleotide from natural abundance ^{13}C-^1H correlated experiments, *J. Am. Chem. Soc.* **113,** 9349–9354 (1991).
10. J. R. Tolman, J. M. Flanagan, M. A. Kennedy, and J. H. Prestegard, Nuclear magnetic dipole interactions in field-oriented proteins—Information for structure determination in solution *Proc. Natl. Acad. Sci. USA* **92,** 9279–9283 (1995).
11. N. Tjandra and A. Bax, Direct measurement of distances and angles in biomolecules by NMR in a dilute liquid crystalline medium, *Science* **278,** 1111–1114 (1997).
12. J. R. Tolman and J. H. Prestegard, Measurement of amide ^{15}N–^1H one-bond couplings in proteins using accordion heteronuclear-shift-correlation experiments, *J. Magn. Reson. B* **112,** 269–274 (1996).
13. N. Tjandra and A. Bax, Large variations in $^{13}C_\alpha$ chemical shift anisotropy in proteins correlate with secondary structure, *J. Am. Chem. Soc.* **119,** 9576–9577 (1997).
14. M. Ottiger, F. Delaglio, and A. Bax, Measurement of *J* and dipolar couplings from simplified two-dimensional NMR spectra, *J. Magn. Reson.* **131,** 373–378 (1998).
15. D. W. Yang, J. R. Tolman, N. K. Goto, and L. E. Kay, An HNCO-based pulse scheme for the measurement of $^{13}C_\alpha$–$^1H_\alpha$ one-bond dipolar couplings in ^{15}N, ^{13}C labeled proteins, *J. Biomol. NMR* **12,** 325–332 (1998).
16. F. Tian, H. M. Al-hashimi, J. L. Craighead, and J. H. Prestegard, Conformation of a flexible oligosacharide using residual dipolar couplings, *J. Am. Chem. Soc.* **123,** 485–492 (2001).
17. P. Andersson, K. Nordstrand, M. Sunnerhagen, E. Liepinsh, I. Turovskis, and G. Otting, Heteronuclear correlation experiments for the determination of one-bond coupling constants, *J. Biomol. NMR* **11,** 445–450 (1998).
18. P. Andersson, A. Annila, and G. Otting, An α/β-HSQC-α/β experiment for spin-state selective editing of IS cross peaks, *J. Magn. Reson.* **133,** 364–367 (1998).
19. P. Andersson, J. Weigelt, and G. Otting, Spin-state selection filters for the measurement of heteronuclear one-bond coupling constants, *J. Biomol. NMR* **12,** 435–441 (1998).
20. B. Brutscher, J. Boisbouvier, A. Pardi, D. Marion, and J. P. Simorre, Improved sensitivity and resolution in ^1H–^{13}C NMR experiments of RNA, *J. Am. Chem. Soc.* **120,** 11,845–11,851 (1998).
21. M. H. Lerche, A. Meissner, F. M. Poulsen, and O. W. Sorensen, Pulse sequences for measurement of one-bond ^{15}N–^1H coupling constants in the protein backbone, *J. Magn. Reson.* **140,** 259–263 (1999).

22. F. Cordier, A. J. Dingley, and S. Grzesiek, A doublet-separated sensitivity-enhanced HSQC for the determination of scalar and dipolar one-bond J-couplings, *J. Biomol. NMR* **13,** 175–180 (1999).
23. G. Griesinger, O. W. Sorensen, and R. R. Ernst, Practical aspects of the E. COSY technique: Measurement of scalar spin–spin coupling constants in peptides, *J. Magn. Reson.* **75,** 474–492 (1987).
24. A. Bax, G. W. Vuister, S. Grzesiek, F. Delaglio, A. C. Wang, R. Tschudin, and G. Zhu, Measurement of homonuclear and heteronuclear J-couplings from quantitative J-correlation, *Methods Enzymol.* **239,** 79–105 (1994).
25. J. R. Tolman and J. H. Prestegard, A quantitative J-correlation experiment for the accurate measurement of one-bond amide N-15-H-1 couplings in proteins, *J. Magn. Reson. B* **112,** 245–252 (1996).
26. D. Neri, G. Otting, and K. Wuthrich, New nuclear-magnetic-resonance experiment for measurements of the vicinal coupling-constants $^3J_{NH,HA}$ in proteins, *J. Am. Chem. Soc.* **112,** 3663–3665 (1990).
27. S. Uhrínová, D. Uhrín, T. Liptaj, J. Bella, and J. Hirsch, Measurement of one-bond proton carbon coupling-constants of saccharides, *Magn. Reson. Chem.* **29,** 912–922 (1991).
28. G. W. Vuister, F. Delaglio, and A. Bax, The use of $^1J(C_\alpha H_\alpha)$ coupling-constants as a probe for protein backbone conformation, *J. Biomol. NMR* **3,** 67–80 (1993).
29. N. Tjandra, S. Grzesiek, and A. Bax, Magnetic field dependence of nitrogen-proton J splittings in ^{15}N-enriched human ubiquitin resulting from relaxation interference and residual dipolar coupling, *J. Am. Chem. Soc.* **118,** 6264–6272 (1996).
30. N. Tjandra and A. Bax, Measurement of dipolar contributions to $^1J_{CH}$ splittings from magnetic-field dependence of J modulation in two-dimensional NMR spectra, *J. Magn. Reson.* **124,** 512–515 (1997).
31. M. Ottiger, F. Delaglio, J. L. Marquardt, N. Tjandra, and A. Bax, Measurement of dipolar couplings for methylene and methyl sites in weakly oriented macromolecules and their use in structure determination, *J. Magn. Reson.* **134,** 365–369 (1998).
32. T. K. Hitchens, S. A. McCallum, and G. S. Rule, A J_{CH}-modulated 2D (HACACO)NH pulse scheme for quantitative measurement of $^{13}C_\alpha$–$^1H_\alpha$ couplings in ^{15}N, ^{13}C-labelled proteins, *J. Magn. Reson.* **140,** 281–284 (1999).
33. T. Rundlof, C. Landersjo, K. Lycknert, A. Maliniak, and G. Widmalm, NMR investigation of oligosaccharide conformation using dipolar couplings in an aqueous dilute liquid crystalline medium, *Magn. Reson. Chem.* **36,** 773–776 (1998).
34. M. Martin-Pastor and C. A. Bush, Conformational studies of human milk oligosaccharides using ^{1}H–^{13}C one-bond NMR residual dipolar couplings, *Biochemistry* **39,** 4674–4683 (2000).
35. M. Martin-Pastor and C. A. Bush, The use of NMR residual dipolar couplings in aqueous dilute liquid crystalline medium for conformational studies of complex oligosaccharides, *Carb. Res.* **323,** 147–155 (2000).
36. H. C. Kung, K. Y. Wang, I. Goljer, and P. H. Bolton, Magnetic alignment of duplex and quadruplex DNAs, *J. Magn. Reson. Ser. B* **109,** 323–325 (1995).
37. R. D. Beger, V. M. Marathias, B. F. Volkman, and P. H. Bolton, Determination of internuclear angles of DNA using paramagnetic assisted magnetic alignment, *J. Magn. Reson.* **135,** 256–259 (1998).
38. A. Vermeulen, H. J. Zhou, and A. Pardi, Determining DNA global structure and DNA bending by application of NMR residual dipolar couplings, *J. Am. Chem. Soc.* **122,** 9638–9647 (2000).
39. J.-R. Brisson, S.-C. Sue, W.-G, Wu, G. McManus, T. N. Pham, and D. Uhrín, NMR of carbohydrates: 1D homonuclear selective methods, *in* "NMR and Glycoconjugates" (J. Jimenez-Barbero and T. Peters, Eds.), Wiley/VCH Verlag, Weinheim, in press (2002).
40. J. R. Garbow, D. P. Weitekamp, and A. Pines, Bilinear rotation decoupling of homonuclear scalar interactions, *Chem. Phys. Lett.* **93,** 504, (1982).
41. D. Uhrín, T. Liptaj, and K. E. Kövér, Modified BIRD pulses and design of heteronuclear pulse sequences, *J. Magn. Reson. A* **101,** 41–46 (1993).
42. A. G. Palmer, J. Cavanagh, P. E. Wright, and M. Rance, Sensitivity improvement in proton-detected two-dimensional heteronuclear correlation NMR spectroscopy, *J. Magn. Reson.* **93,** 151–170 (1991).
43. L. E. Kay, P. Keifer, and T. Saarinen, Pure absorption gradient enhanced heteronuclear single quantum correlation spectroscopy with improved sensitivity *J. Am. Chem. Soc.* **114,** 10,663–10,665 (1992).
44. O. W. Sorensen, G. W. Eich. M. H. Lewitt, G. Bodenhausen, and R. R. Ernst, Product operator formalism for description of NMR pulse experiments, *Prog. NMR Spectrosc.* **16,** 163–192 (1983).
45. P. Sándor, G. A. Morris, and A. Gibbs, Iterative analysis of strong coupling effects in semiselective J spectroscopy, *J. Magn. Reson.* **81,** 255–261 (1989).
46. C. Morat, F. R. Taravel, and M. R. Vignon, Long-range proton–carbon-13 coupling constants of monosaccharides by selective heteronuclear 2D-J NMR spectroscopy, *Magn. Reson. Chem.* **26,** 264–270 (1988).
47. G. M. Clore, M. R. Starich, and A. M. Gronenborn, Measurement of residual dipolar couplings of macromolecules aligned in the nematic phase of a colloidal suspension of rod-shaped viruses, *J. Am. Chem. Soc.* **120,** 10,571–10,572 (1998).
48. A. Bax and T. C. Pochapsky, Optimized recording of heteronuclear multidimensional NMR spectra using pulsed field gradients, *J. Magn. Reson.* **99,** 638–643 (1992).